APPENDIX 3F: Precision and Accuracy of Optical Measurements

3F.1 Accuracy of Extinction and Scattering Measurements

Introduction

Measurement of the extinction coefficient is essential to understanding how atmospheric aerosols affect the visibility of scenic vistas. However, accurate measurement of extinction in clean atmospheres and under all meteorological conditions poses a formidable problem. To date, the two methods routinely employed for estimating extinction are integrating nephelometry and teleradiometry using natural targets.[1, 2] Both measurement techniques have serious shortcomings. The integrating nephelometer measures atmospheric scattering and not absorption, may modify particles that pass through its sampling chamber and properly measures scattering from only fine particles. Calculations of atmospheric extinction using teleradiometer measurements of natural target contrast, on the other hand, are sensitive to both scattering and absorption, and measure effects of particles of all sizes in the ambient aerosol. However, the extinction calculation from the contrast measurement is sensitive to variations in inherent contrast and nonuniform illumination conditions, neither of which can be readily accounted for in normal measurements.[3]

A transmissometer operated without enclosing the light beam has the potential for measuring atmospheric extinction without perturbing the aerosols and without the inadvertent removal of large ($\gtrsim 10\mu m$) aerosols by a closed chamber inlet. However, transmissometers with path lengths greater than a few kilometers are required to achieve the sensitivity to measure extinctions near the Rayleigh limit. Operation of transmissometers over path lengths greater than 2–3 km can result in beam modification because of atmospheric turbulence effects. Beam 'spreading' results in a lower detected beam irradiance that is erroneously interpreted as atmospheric extinction.

From 1985 to 1988 the National Park Service (NPS) carried out a number of tests on a long path transmissometer manufactured by OPTEC, Inc.[4] One transmissometer design criteria was to measure atmospheric extinction in near Rayleigh atmospheres to an accuracy of better than 10%. Since standard atmospheres and/or gases cannot be introduced into open air long path instruments, a number of field programs were designed to intercompare the transmissometer with itself but with different path lengths and with other atmospheric extinction/scattering measurement techniques. Under certain limiting conditions various measurement techniques will accurately measure atmospheric scattering and/or extinction and consequently should compare favorably.

Intercomparisons included side by side operation of two transmissometers with path lengths of 5.79 km and 15.57 km. Unless the effect of atmospheric turbulence on derived extinction has a specific functional form, it is expected that as the path length is increased, the error due to turbulence

on measured extinction will increase. Thus, the deviation between two extinction measurements made over different path lengths may yield some insight into the accuracy of the measurement or the functional form of the effect that turbulence is having on derived extinction.

A second field study compared transmissometer derived extinction with an extinction calculated from teleradiometer sky-target contrast measurements of an artificial black target. By fabricating a target with $C_o = -1.0$, the error associated with uncertain inherent contrast resulting from uneven illumination of the target or clouds behind the target are eliminated. However, some error associated with clouds shading the sight path still remain.[3]

In each of the above described experiments and as part of a special winter 1986 study, the transmissometer was compared to integrating nephelometer measurements of the atmospheric scattering coefficient. Under near Rayleigh conditions or when the atmosphere is free of absorbing and large particles and the RH is less than approximately 60%, nephelometer scattering coefficient measurements should compare favorably to transmissometric derived atmospheric extinction.

Comparison of the Two Transmissometers Operated Over Different Path Lengths

The objective of operating two transmissometers side by side but with different path lengths was to investigate the effect of atmospheric turbulence on transmissometer-derived atmospheric extinction. The instruments were operated at Grand Canyon, Arizona from late May to the end of July 1986. One instrument was operated continuously over a 5.79 km path, while a second instrument, configured to make 10 minute average readings at the top of each hour, had a path length of 15.57 km. Both receivers were placed at Grand View Point with the transmitters located at Moran Point (5.79 km) and Desert View Watchtower (15.57 km). To minimize turbulence due to thermal gradients near the surface of the ground, instruments were placed next to cliff edges such that the light beam path was well above terrain features.

To examine the relationships between extinction derived from the two instruments, a scatterplot, shown in Figure 3F.1, was made with the 15.57 km and 5.79 km path instruments plotted on the x and y axes, respectively. The continuous signal from the 5.79 km instrument was averaged to correspond to the 15.57 km instrument. Pertinent statistics associated with Figure 3F.1 are presented in Table 3F.1.

The two instruments compared quite favorably. It is clear that there is an approximate linear relationship between the two extinction coefficients. Correlations between $b_{ext,1}$ and $b_{ext,2}$ are equal to 0.97, and a perpendicular departure regression analysis indicates a straight line with nonsignificant intercept. (See Appendix 3G for discussion of perpendicular regression.) 95% of the time b'_1 is within 13% of b'_2, while relative error between b'_1 and b'_2, given by

$$RE = \frac{1}{n}\sum[|b_{1i} - b_{2i}|/(b_{1i} + b_{2i})/2] \qquad (3F.1)$$

averaged over all cases is 11.6%. That is, the discrepancy between the two transmissometers is 11.6% on the average. In fact, in 75% of the cases the discrepancy is less than or equal to 4.3%.

The rather exceptional agreement between the two instruments under a variety of turbulence conditions and during day and nighttime conditions suggests that either turbulence was not significantly affecting the transmissometer-derived extinction calculation and that the transmissometers were making very accurate measurements or that the effect of atmospheric turbulence on measured irradiance takes on the form of Equation 3A.8 and the effects of turbulence are not detected by this experiment.

Table 3F.1: Pertinent statistics for comparing the transmissometer derived extinction to other measures of extinction/scattering.

	Slope	Intercept	SE of Slope	SE of Intercept	R
Transmissometer 1 *vs* Transmissometer 2 (Summer 1986)	0.97	0.0002	0.016	0.000	0.98
Transmissometer *vs* Black Box	1.07	–0.003	0.074	0.003	0.80
Transmissometer *vs* Nephelometer (Grand Canyon)	0.91	0.0007	0.027	0.001	0.94
Transmissometer *vs* Nephelometer (Meteor Crater)	0.60	0.001	0.06	0.002	0.79
Transmissometer *vs* Nephelometer (WHITEX, Page, 10 minute)	0.44	0.010	0.013	0.000	0.75
Transmissometer *vs* Nephelometer (WHITEX, Page, 6-hour)	0.43	0.011	0.020	0.001	0.84
Transmissometer *vs* Nephelometer (WHITEX, Page, 10 minute, RH $\geq$ 60%)	0.38	0.012	0.014	0.001	0.80
Transmissometer *vs* Nephelometer (WHITEX, Page, 6-hour, RH $\geq$ 60%)	0.38	0.013	0.029	0.001	0.84
Transmissometer *vs* Nephelometer (WHITEX, Page, 10 minute, RH < 60%)	1.22	-0.007	0.054	0.001	0.66
Transmissometer *vs* Nephelometer (WHITEX, Page, 6-hour, RH < 60%)	0.82	0.002	0.059	0.001	0.78

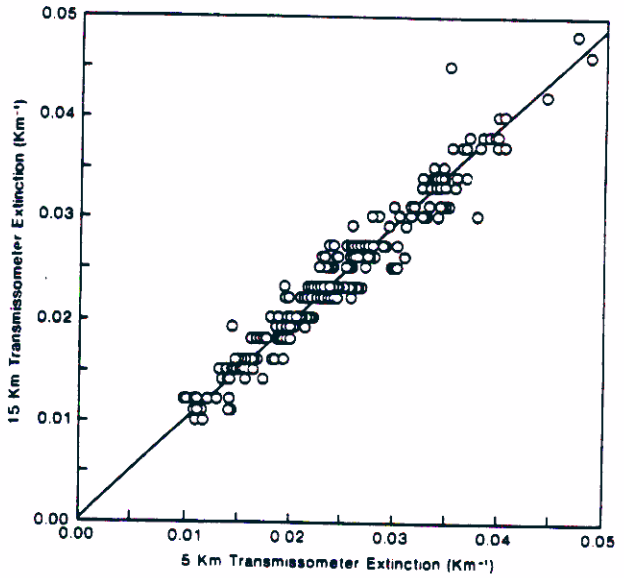

Figure 3F.1: Comparison of extinction coefficients derived from transmissometers operated over two different path lengths.

Comparison of Transmissometer Extinction to Teleradiometer Black Target Extinction

Teleradiometers measuring atmospheric radiance of sky and natural targets can be used in a number of ways to yield approximations of atmospheric extinction.[3] However, the traditional method of making teleradiometric extinction measurements involves measuring sky and natural target radiance at some distance r and using:

$$C_r = C_o \frac{{}_sN_o}{{}_sN_r} e^{-\bar{b}_{ext} r} \tag{3F.2}$$

to approximate b_{ext}.[3] C_r and C_o are the apparent and inherent target contrasts respectively, ${}_sN_o$ and ${}_sN_r$ are the sky radiance at the target and observer, while r is the distance to the target and b_{ext} is the average atmospheric extinction coefficient over path length r. If it is assumed that ${}_sN_o/{}_sN_r \approx 1$, then Equation 3A.1 can be solved for b_{ext};

$$\bar{b}_{ext} = -\frac{1}{r} \ln[C_r/C_o] \tag{3F.3}$$

When using a fabricated black target with $C_o \equiv -1.0$, most errors associated with calculating extinction from contrast measurements under standard illumination conditions are removed. The only error associated with the extinction calculation is due to the uncertainty in ${}_sN_o/{}_sN_r$. For standard illumination conditions over the short path lengths ($r < 10$ km) required for use of artificial black targets, ${}_sN_o/{}_sN_r \approx 1$ and little error is associated with determining extinction.[3] However, single teleradiometer contrast measurements of black targets are still subject to cloud shadowing of the sight path which results in ${}_sN_o \neq {}_s N_r$. Errors due to sight path shadowing can

only be remedied by measuring sky radiance at the target ($_sN_o$) and explicitly accounting for the ratio $_sN_o/_sN_r$.

In the field experiment using black targets the target teleradiometer distance was 3.3 km. A sensitivity analysis of path radiance as a function of target distance shows that the teleradiometer's accuracy and sensitivity must be extremely high. For a black target located 3.3 km distant from the teleradiometer, the path radiance on a Rayleigh day will be approximately 3.5% of the sky radiance. To measure Rayleigh extinction (0.01 km^{-1}) with an accuracy of near 10% requires a contrast measurement accuracy of less than 1/2%. Therefore, special care must be taken to carefully characterize teleradiometer flare characteristics. Measurements showed that teleradiometer flare was nearly 1% of background sky radiance. Therefore the path radiance readings were corrected for flare using:

$$_tN_{3.3km} =_t N'_{3.3km} - 0.01_sN_{3.3km} \qquad (3F.4)$$

where $_tN'_{3.3km}$ is the measured path radiance, $_sN_{3.3km}$ is the measured sky radiance at the observation point, and $_tN_{3.3km}$ is the corrected path radiance used to calculate the extinction coefficient. The subscript 3.3 km indicates that the artificial target was 3.3 km from the observation point.

Other considerations in using artificial black targets are the required target size as a function of target distance and the problem of maintaining teleradiometer alignment on the black portion of the target. For instance, the teleradiometer used in the field study was designed with a 0.017° angle of view. This corresponds to an approximate 1.0 m target at a path distance of 3.3 km. For purposes of maintaining alignment and reducing teleradiometer flare, the target was chosen to be twice as big or approximately 2.0 m in diameter.

When the teleradiometer is aligned so that it is centered on the black target, a shift in alignment of only 0.0085° moves the teleradiometer off target. Therefore, alignment was routinely checked to minimize drift in teleradiometer positioning.

During October 1985, a study was conducted near Meteor Crater, Arizona to intercompare a number of methods for measuring atmospheric extinction. As part of that experiment, a precision, low-flare teleradiometer was used to measure contrast of a prefabricated two meter diameter black target located 3.3 km from the observation point. All teleradiometers used in the black target experiment were calibrated to yield identical readings (millivolts) when measuring the radiant energy from a constant radiance light source. Relative radiance is defined to be teleradiometer voltage output. The actual radiance can be achieved by multiplying the teleradiometer voltage by an appropriate constant. However, for purposes of this experiment, absolute radiance is not necessary since the constant will cancel out when calculating contrast.

Figure 3F.2 shows a plot of the October 9, 1985 "raw" teleradiometer readings associated with the artificial black target. The highest readings correspond to sky radiance, while the lower readings correspond to the path radiance between the observation point and black target. The "relative radiance" reading for the path radiance can be arrived at by dividing the y-axes scale in Figure 3F.2 by a factor of 2. From the hours 0000 to 0600 and 1800 to 2400 the sun is down and the teleradiometer reads zero radiance. The effects of clouds on lighting conditions are reflected in teleradiometer readings between 0600 and 1200 hours. From 1200 to 1400 hours there were intermittent showers with enough rain during 1200 to 1300 hours to make teleradiometer readings drop to near zero at certain times. These readings were eliminated from the data set. Afternoon readings correspond to nearly cloud-free conditions. Notice how the sky and path radiance varies smoothly in time. The increase in path radiance at 1600 hours corresponds to an increase in particulate matter which was also measured by the transmissometer and nephelometer. The teleradiometer relative radiance readings were converted to atmospheric extinction through the use of Equation 3F.3 after correcting for flare.

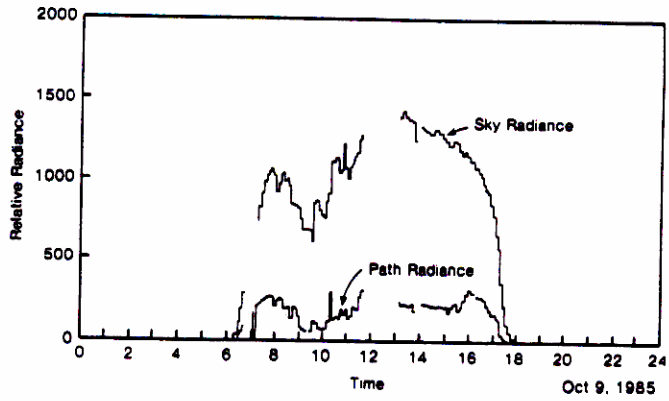

Figure 3F.2: Relative sky and path radiance for the black target experiment plotted as a function of time for October 9, 1985. Relative path radiance is equal to the y-axis relative radiance values divided by two.

Adjacent to the black target instrumentation, a transmissometer was operated over a path length of 8 km. The instrument was calibrated by the same method as previously described. Figure 3F.3 is a scatterplot comparing "black target" to transmissometer extinction for all data gathered during the study period. Slopes of the regression line comparing two measurements were carried out using "perpendicular" departure rather than conventional regression analysis since there is error in both dependent and independent variables.[5]

The slope of the regression line is equal to 1.07 ± 0.074 and the intercept (-0.003 ± 0.003) is not statistically different from zero. The correlation between the two measurements is 0.80 while the relative error is 15.0%. Given the potential error due to sight path shading by cloud cover, the agreement between the two instruments is surprisingly good.

3F.1.1 Comparison of Transmissometer Extinction to Integrating Nephelometer Scattering

This section will compare the extinction measurements by OPTEC transmissometers with scattering measurements by MRI integrating nephelometers. The conclusion will be made that the two instruments agree well at low humidity ($RH < 70\%$), but disagree at high humidity, with the nephelometer giving considerably lower values. For this comparison, it is important to remember that the average absorption coefficient during WHITEX was approximately 20% of the scattering coefficient. In this environment, the nephelometer would be expected to have scattering coefficients that are approximately 80% of the extinction coefficients by the transmissometer.

The integrating nephelometer differs conceptually from the methods discussed above in that it measures the light scattered from the aerosol, whereas the other methods measure a change in radiance or transmittance due to scattering and absorption. The geometry of the instrument is such (see, for example, the description in reference 1) that the signal is proportional to the scattering portion of b_{ext}, namely b_{scat}. This is an advantage in clean environments, because a small quantity is measured directly rather than being derived from a difference or ratio of larger numbers and, in

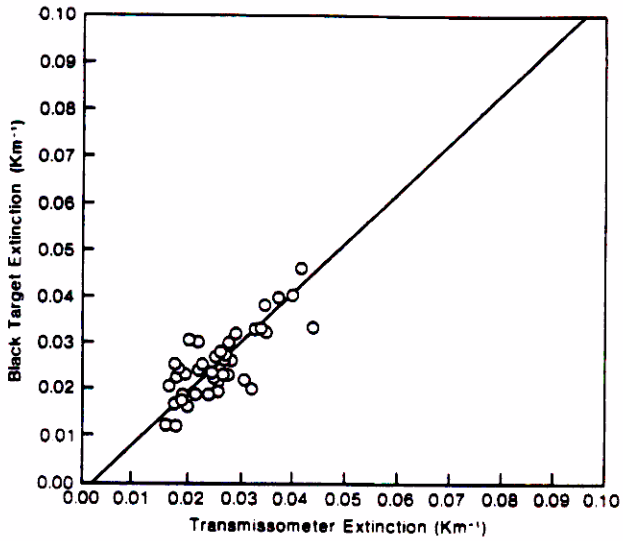

Figure 3F.3: Scatterplot of black target and transmissometer atmospheric extinction. The slope of the perpendicular regression line is equal to 1.07 ± 0.074 and the intercept is equal to −0.003 ± 0.003.

fact, commercially-available integrating nephelometers can reliably measure b_{scat} due to Rayleigh scattering from gases. On the other hand, the optical signal is so small that it has been measured most successfully in a totally dark, closed chamber, free of stray light.

The closed chamber and instrument geometry result in several considerations concerning the use of the instrument for determining atmospheric extinction:

- The measurements are totally independent of meteorological conditions and illumination, and they directly measure one component of extinction independent of atmospheric lighting conditions.
- The measurement is made at one point in space and thus can be compared unambiguously to particulate data that is also gathered at the same point.
- The sample must be drawn through ducts into a chamber which, in practice, is a different environment from the ambient. This can result in modification of the aerosol due to impaction on surfaces and because of heating or cooling.
- The commercially available instrument used in the field studies (MRI 1560) inadvertently heated the sample by approximately 10°F. However, heating can be minimized to about 1°–2° with special modifications of the instrument.
- The commercially available instrument is unable to measure light scattering in the extreme forward and backward directions, typically within 8–10° of the axis. For particles larger than a few micrometers in diameter, a substantial fraction of the scattering is in the forward direction and is not detected by the nephelometer, which means that the instrument underestimates the scattering from larger particles.

The errors caused by the various factors noted above vary from location to location. Heating of the sample by the instrument, by even a few degrees Celsius, can cause errors approaching 100%

at high humidities when the particles deliquesce.[5, 6] Forward angle truncation typically results in about 10% underestimates[7, 8] (after allowing for the fact that calibration of the instrument with a Rayleigh scattering gas compensates for some of the truncation error).

In the field studies at Grand Canyon and Meteor Crater, the MRI 1560 integrating nephelometer was used. The instrument was operated according to standard procedures. The span of the instrument was set using Freon 12, while the "zero" point was monitored at least every six hours by pumping clean air through the sampling chamber. Typical temperature differences between the nephelometer inlet and outlet were around 10°F.

At Grand Canyon, the nephelometer was operated at Hopi Point, a monitoring site which is approximately 18 kilometers from Grand View Point and 30 kilometers from Desert View. Figure 3F.4 shows a scatterplot of hourly average nephelometer and 5.79 km transmissometer scattering/extinction measurements. Given the rather large physical separation of the two instruments and the fact that the operation logbook indicated some local control burn activity, the instruments compared favorably. The perpendicular regression line slope is 0.91 ± 0.27, with a near zero intercept of 0.00068 ± 0.001, while the correlation coefficient is 0.94. When the atmosphere is free of aerosols, both instruments should predict Rayleigh scattering of 0.01 km^{-1}. The regression equation can be used to estimate relative error (RE) by predicting b_{ext} when $b_{scat} = 0.01$. The RE is given by $(b_{scat,R} - b_{ext,R})/0.01$ where $b_{scat,R}$ and $b_{ext,R}$ are the nephelometer and transmissometer Rayleigh scattering coefficients. The RE for the Grand Canyon experiment was 9.9%. On the average, however, the nephelometer predicted scattering coefficient was approximately 10% lower than transmissometer extinction. The difference could be attributed to nephelometer underestimation of large particle scattering, absorption or drying of wet aerosols.

A similar comparison was done during the Meteor Crater study and results are shown in a scatterplot presented in Figure 3F.5. The slope of the perpendicular regression line for this study was 0.60 ± 0.06 and the intercept again was near zero at 0.001 ± 0.002. The correlation between the two measurements is near 0.80 while the relative error is 30% at Rayleigh conditions. A slope of 0.60 implies that on the average nephelometer scattering was approximately 50% lower than transmissometer-derived extinction.

Transmissometers and integrating nephelometers were operated side-by-side during WHITEX at Canyonlands, Hopi Point, and Page. Figure 3F.6 shows the ratio of 10-minute transmissometer measurements of extinction to the corresponding nephelometer scattering measurements at Page for the time period of February 6–13. Below $RH = 70\%$, the ratio is approximately 1. Above 70%, the ratio rises sharply, with the nephelometer giving lower measurements.

The transmissometer and nephelometer measurements were averaged over each 6-hour period, in order to minimize inhomogeneous aerosol distributions and to allow comparison to the 6 and 12-hour measurements of particulate and gaseous variables. The Page comparisons for 10-minute and 6-hour averages in Table 3F.1 show that the longer integration time gives similar slopes and intercepts but better r^2. Figure 3F.7 shows the ratio of transmissometer/nephelometer as a function relative humidity for all 6-hour averages. As before, the two measurements differ for high relative humidity, although the difference is less pronounced than that for the 10-minute measurements at Page. Note that there is a small slope even below 70%, indicating that the processes causing lower nephelometer readings may have a small effect even at moderate relative humidity.

Figure 3F.8 shows comparisons of the transmissometer and the nephelometer for relative humidity either above or below 70%. For relative humidity below 70% (upper plot), the intercept is near zero ($\pm 2\sigma$) and the slope is near the expected 0.8. For relative humidity above 70%, the slope is much less than 0.8 and the intercept is not zero.

Two possible mechanisms could explain the underestimation by the integrating nephelometer at high humidity. The first mechanism involves the temperature increase in the sampling chamber

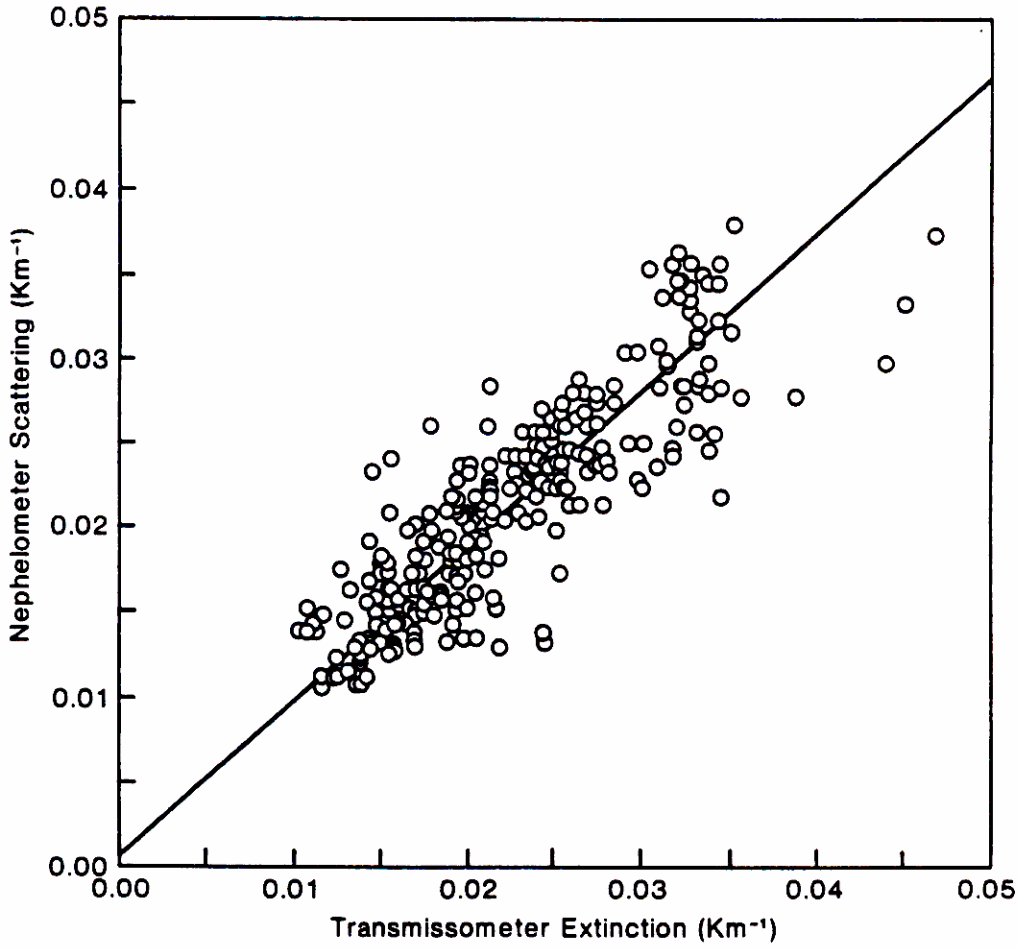

Figure 3F.4: Scatterplot of hourly averaged nephelometer scattering and transmissometer extinction for the Grand Canyon intercomparison study. The slope of the perpendicular regression line is equal to 0.91 ± 0.027 and the intercept is equal to 0.0007 ± 0.001.

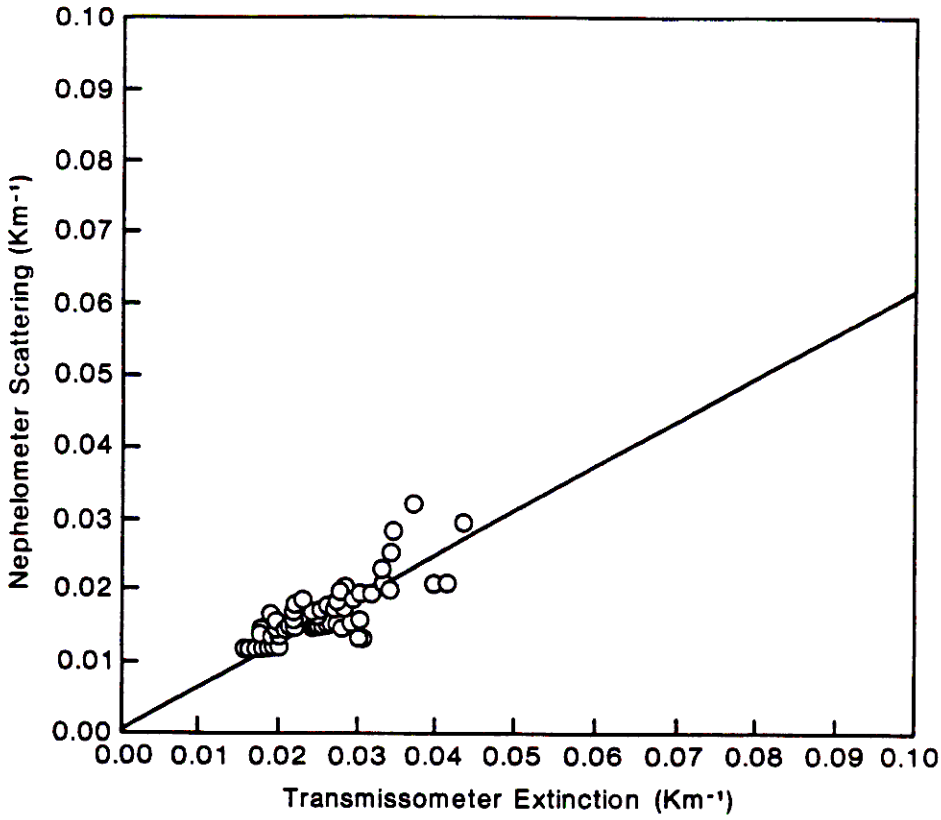

Figure 3F.5: Scatterplot of "daytime" hourly averaged integrating nephelometer scattering and transmissometer extinction for the Meteor Crater study. The slope of the perpendicular regression line is 0.60 ± 0.06 and the intercept is equal to 0.001 ± 0.002.

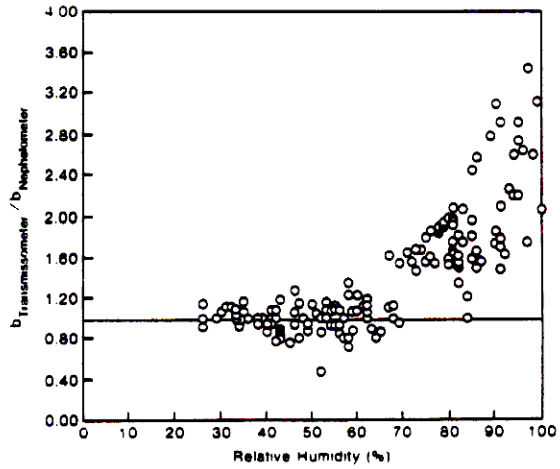

Figure 3F.6: Ratio of the 10 minute transmissometer extinction to nephelometer scattering as a function of relative humidity. Data is from Page for February 6–13. The horizontal line corresponds to a ratio of 1.0.

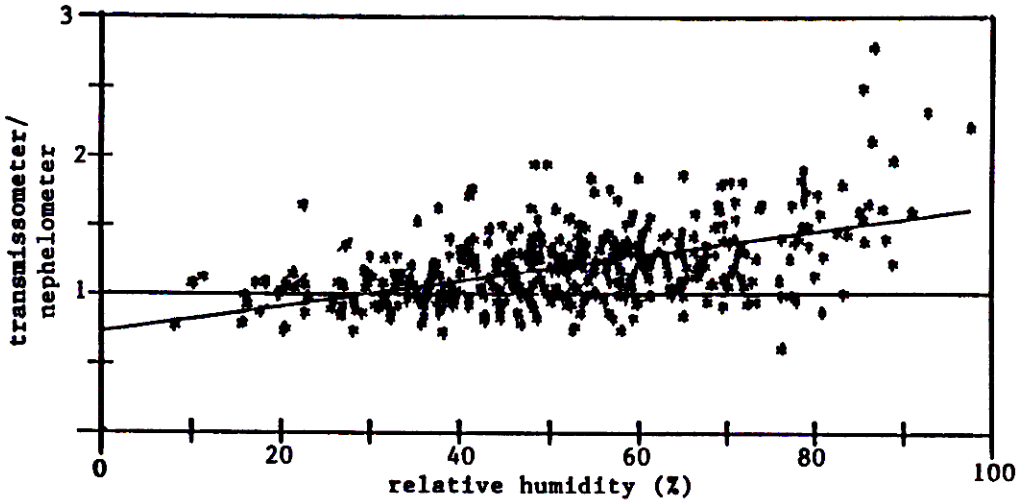

Figure 3F.7: The ratio of 6-hour transmissometer extinction to nephelometer scattering as a function of relative humidity. All WHITEX sites and time periods.

air of approximately 5°C. The second mechanism is based on the forward angle truncation of the integrating nephelometer caused by baffles needed to block the light beam; the detection efficiency drops linearly from 100% at around 20° to 0% at around 4°. Both mechanisms use the fact that hydroscopic particles, such as ammonium sulfate, will grow in size as the humidity increases from around 0.3 μm to around 0.5 μm, thereby increasing the efficiency for total scattering by a factor of 2.

The temperature mechanism assumes that the heating of the air will cause the particles to lose water and decrease in size. Since the total scattering efficiency is decreased, the value measured by the nephelometer will decrease. The second mechanism was suggested by studies of the angular distribution of the scattering conducted with the UCD polar nephelometer. As the particles increase in size from 0.3 μm, not only does the total scattering efficiency increase, but a larger fraction of the scattering is contained in the forward angles. Since the integrating nephelometer is less efficient at measuring forward angle scattering, it will underestimate the coefficient for 0.6 μm particles more than that for 0.3 μm particles. Further tests are being conducted to determine if the decrease in the nephelometer reading can be predicted quantitatively.

Conclusion

Three separate field studies were conducted to examine the ability of the OPTEC, Inc. transmissometer to measure atmospheric extinction. One study sought to investigate the effect of atmospheric turbulence by operating two identical transmissometers over two path lengths. If turbulence is causing the measured irradiance to be erroneously low, the effect should manifest itself more for longer than shorter paths. A second study compared transmissometer extinction to teleradiometer black target contrast derived extinction. Using a truly black target eliminates all the error associated with uncertainty in inherent contrast. Finally, the transmissometer extinction was compared to nephelometer scattering. It is expected under some circumstances that nephelometer scattering and transmissometer extinction should compare favorably. For instance, in clean atmospheres both instruments should measure the Rayleigh scattering coefficient. All of the above measurements

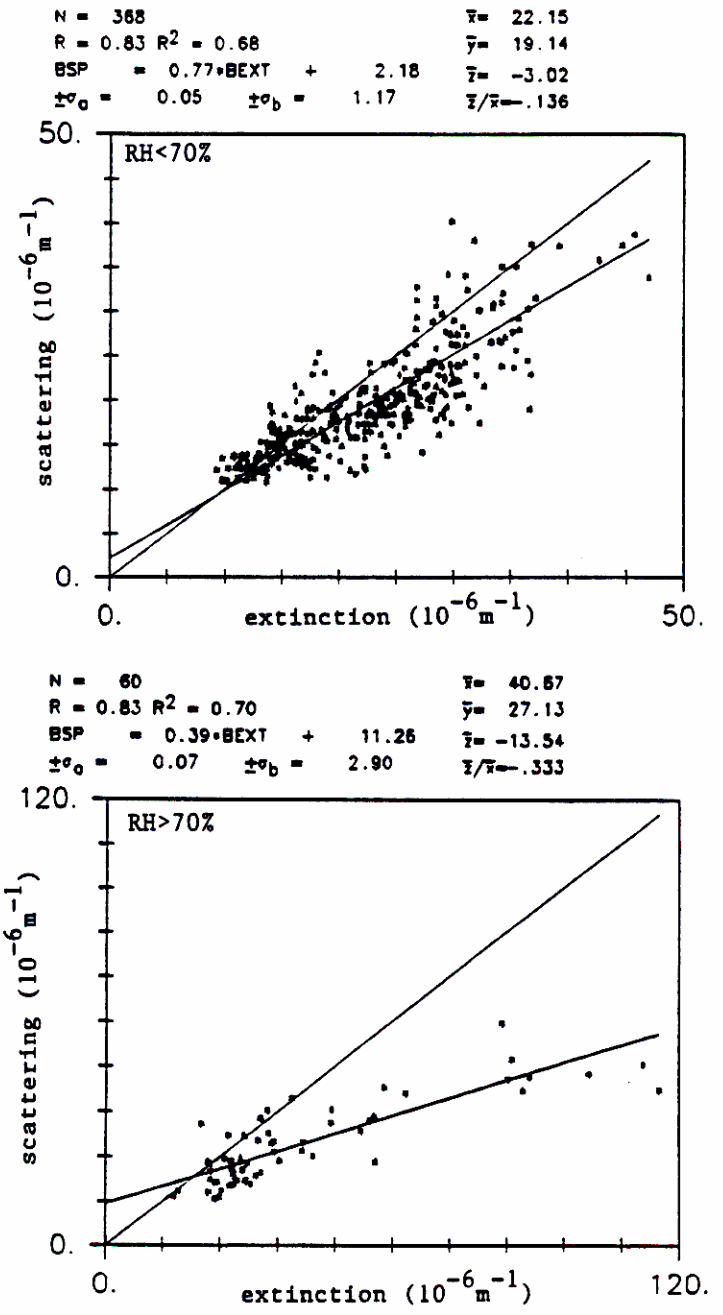

Figure 3F.8: Comparison of 6-hour transmissometer extinction and nephelometer scattering for relative humidity below 70% (upper plot) and above 70% (lower plot). All WHITEX sites and time periods.

suggest that the transmissometer is accurately measuring the true unperturbed ambient extinction coefficient. Specifically:

- Two transmissometers operating under a variety of turbulence conditions, both day and night but over different path lengths, yielded almost identical extinction, indicating the turbulence did not affect the measurements or that turbulence effects on measured irradiance is a very simple exponential function of the path length r. The average relative error between the two instruments was 11.6%

- The transmissometer and black target extinctions correlated very well and there was little apparent bias between the two instruments. The linear regression line between the two variables was not statistically different from one. The average relative error was 15.0%

- In each of the studies, nephelometer scattering was systematically lower than transmissometer extinction by as little as 10% and in some cases by as much as 80% under others. However, the intercept of the regression line comparing the two instruments had an intercept (except for RH > 60% at Page, AZ), which was not substantially different from zero, indicating atmospheric turbulence was not affecting the transmissometer measurements. If the transmissometer readings are being biased toward higher extinctions because of atmospheric turbulence, it would be expected that this bias would be apparent on Rayleigh as well as high extinction periods. The average relative error between the transmissometer and nephelometer measured Rayleigh scattering was 9.9%, 30% and 9.0% at Grand Canyon, Meteor Crater and Page, respectively.

3F.2 Precision and Accuracy of Absorption Measurements

Introduction

The optical parameters have proven to be more difficult to measure than was originally though. Section 3F.1 showed that the integrating nephelometer has difficulties when the humidity exceeds around 70%. Several generations of instruments have tried to measure extinction. The determination of the coefficient of absorption by the integrating plate method has also had a controversial history. On the one hand, the LIPM measurement can be highly precise. In the current IMPROVE network, the analytical precision of the UCD LIPM system is 1% to 4$ from moderately light ($1 \times 10^{-6}\ m^{-1}$) to black samples ($20 \times 10^{-6}\ m^{-1}$). On the other hand, side-by-side comparisons by different laboratories often yield different results, depending on the filter and loading. In the accuracy sections below, these problems are shown to be associated with (1) large-angle particle scattering and subtle interactions between the particles and the filters, and (2) shadowing effects that are inherent when attempting to determine the atmospheric coefficient by measuring the absorption of particles on a filter.

Precision

The coefficient was calculated from the intensities of light transmitted through the filter before collection (I_o) and after collection (I), according to

$$b = (\text{area/volume}\ (F) \log_e(I_o/I), \tag{3F.5}$$

where F is the correction term associated with accuracy, to be discussed below.[9] For the WHITEX data, this F term varied from 1.0 for lightly loaded samples to 1.7 for heavily loaded samples.

The precision of each intensity measurement was determined by repeated reanalysis of a series of blank and exposed control filters at the beginning and end of each analysis session. At the time of WHITEX, the standard deviation, σ_I, was 4 intensity units, independent of the measured intensity. The intensities ranged from 350 units for a blank filter to 200 units for the blackest filter. The absolute and relative analytical precisions are

$$\sigma(b) = \left(\frac{\text{area}}{\text{volume}}\right)(F)(\sigma_I)\sqrt{I_o^{-2} + I^{-2}} \tag{3F.6}$$

$$f(b) = \frac{(\sigma_I)\sqrt{I_o^{-2} + I^{-2}}}{\log_e(I_o/I)}. \tag{3F.7}$$

The approximate values of these analytical precisions are shown in Figure 3F.9, based on estimated F factors. The actual calculations for each coefficient are based on the measured areal densities. The average value of the coefficient for the primary sites, $4.2 \times 10^{-6} m^{-1}$.

Figure 3F.10 shows a comparison between 3 samplers. The measured precision of 2% is less than predicted.

Accuracy: Large-Angle Scattering by Particles[9]

The procedures of measuring the intensity of transmitted light before and after collection compensates for the absorption and scattering of the filters material. However, if the particles in the sample scatter any light outside the integrating plate, then the calculated absorption will be larger than the actual absorption. There could also be interference between the particles and the filter, such as penetration of the filter. These effects were tested by comparing the results from the integrating plate system to those from an integrating sphere system. The UCD system, LISA (Laser Integrating Sphere Analyzer), measures both total reflectance and total transmission. Therefore, it determines the absorption without the large-angle scattering assumption. Two significant results were obtained from LISA. First, the Teflon filters do not absorb light; the opacity is caused only by scattering. Second, the apparent absorption measured by LIPM is only a few percent higher than the actual absorption measured by LISA. Figure 3F.11 shows that the LIPM values are approximately 3% higher than LISA. The WHITEX coefficients were multiplied by 0.97 to compensate for this effect, although the correction was smaller than the analytical precision. Since the magnitude of the correction was small, we assumed that the uncertainty in the correction was negligible.

This comparison between LISA and LIPM indicates that large-angle scattering is not a significant problem with Teflon filters. It also indicates that there are no significant accuracy problems associated with interactions between the particles and the filter. LIPM measurements with quartz filters are very difficult because of the very large scattering and absorption by the clean filter. Nuclepore filters have the problem that they collect so little material before clogging.

Accuracy: Shielding by Other Particles on the Filter[9]

In the atmosphere, the light wave reforms after each scattering and absorption interaction, so that each absorbing particle interacts with the incident light. When the particles are collected on the filter, the light wave is not able to reform, so that an absorbing particle could be shielded from the incident light by other particles or the detector could be shielded from the absorbing particle. This effect will be minimal with a lightly loaded sample and will increase with areal density. The effect will be the same for LISA and LIPM.

One way to solve the problem would be to operate only in the region of low areal densities. However, we are generally restricted to analyzing the same filter used for elemental analysis, which

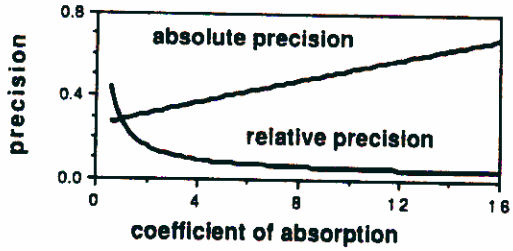

Figure 3F.9: Analytical precision for the coefficient of absorption by LIPM. The units are $10^{-6}m^{-1}$.

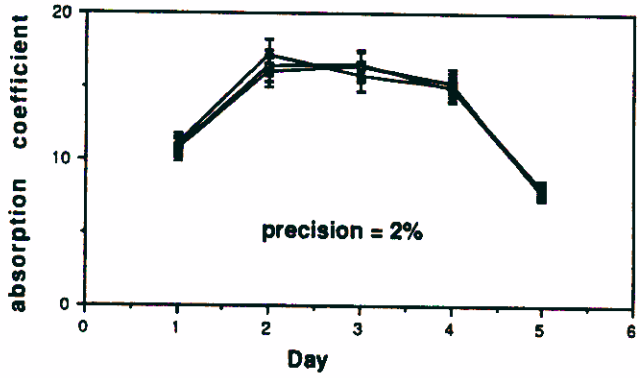

Figure 3F.10: Total precision for the coefficient of absorption by LIPM from side-by-side measurements with three IMPROVE samplers taken at Davis Field Station. The measured precision of 2% is less than predicted. The units are $10^{-6}m^{-1}$.

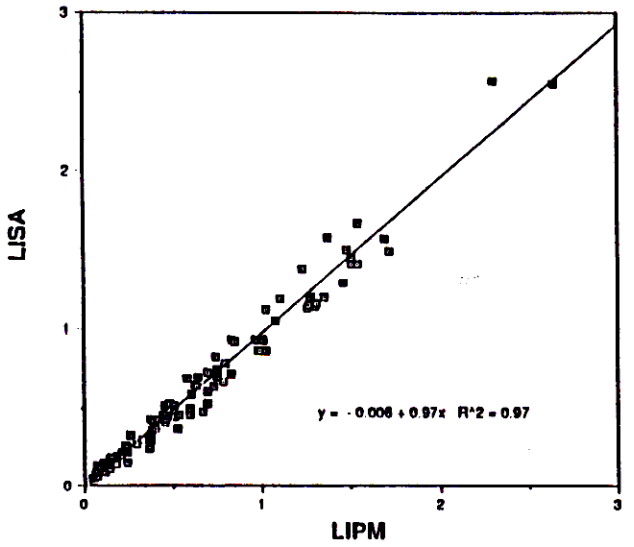

Figure 3F.11: Comparisons of measurements of the coefficient of absorption by LIPM and LISA. The variables are dimensionless numbers before multiplication by (area/volume).

require relatively high areal densities for sensitivity. In addition, the low areal densities are accompanied by large relative LIPM uncertainties. We are thus left with the need to operate in a range requiring a correction.

The shielding correction was estimated by making side-by-side measurements of the same aerosol with filters of different areal densities. Generally, this was accomplished by varying the collection areas by masking. Care was taken to avoid systematic analytical biases caused by different sample areas. We fit the data to a model with two exponentials. The best fit for all data is shown in Figure 3F.12. The correction is given by

$$R = 0.36e^{-\rho t/22} + 0.64e^{-\rho t/415}, \tag{3F.8}$$

where ρt is the areal density of all particles in $\mu g/cm^2$. These WHITEX measurements were corrected by dividing by this factor. For the average mass concentration, the correction was 0.76; for the highest areal density, the value was 0.57.

We estimate the uncertainty of this R factor to be 10% of $1 - R$. Thus the relative accuracy is

$$f(R) = 0.1\left(\frac{1-R}{R}\right). \tag{3F.9}$$

The largest relative uncertainty in R was 7%.

The F factor in equation 3F.5 combines the factors from the two accuracy corrections:

$$F = \frac{0.97}{0.36e^{-\rho t/22} + 0.64e^{-\rho t/415}}. \tag{3F.10}$$

The total uncertainty in b used in the data base was the quadratic sum of analytical precision (equation 3F.7), accuracy (equation 3F.10), and flow rate precision (3%).

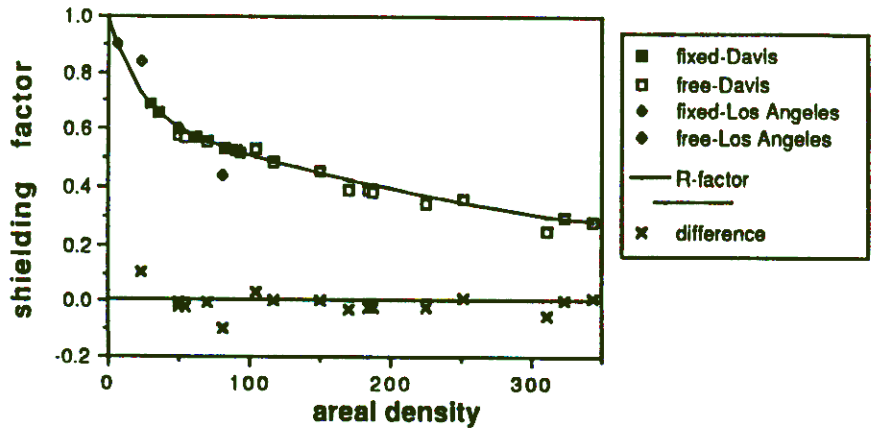

Figure 3F.12: Shielding correction for the coefficient of absorption for samples on a filter. Ratio of measured absorption to ambient absorption. The units of areal density are $\mu g/cm^2$.

Comparison of LIPM with Light-Absorbing Carbon

Figure 3F.13 compares the coefficient4 of absorption by LIPM and the concentration of elemental carbon by the TOR method at Page. The diagonal line corresponds to an absorption efficiency of $10 m^2/g$. Based on the slope, the efficiency is 7 ± 3 m^2/g, and based on the average values, it is 11 ± 1 m^2/g. The correlation is poor, perhaps because of the large uncertainty in LAC, but the slope is reasonable and the intercept is less than 2σ from zero. A somewhat better fit was obtained between ABS by LIPM and LAC by TOR for samples collected in Denver, when the concentrations were much higher and the elemental carbon was dominated by diesel emissions.[10] For diesel emissions, an efficiency of 8–9 m^2/g is expected. However, the efficiency of absorbing particles in wood smoke emissions is not known, although it would probably be slightly higher than 9, if wood smoke particles are less dense. Note that comparing the coefficient of absorption to the elemental carbon by TMO would predict an efficiency of 1–2 m^2/g.

Comparison of LIPM with Transmissometer and Nephelometer

Appendix 3F.1 showed that the scattering coefficient by nephelometer was approximately 0.8 times the extinction coefficient by transmissometer, for relative humidity less than 70%. Figure 3F.14 compares the sum of the scattering and absorption coefficients to the extinction coefficient. For lower relative humidity, the slope is approximately 1σ above 1.0, and the intercept within 1σ of zero. For relative humidity above 70%, the sum of scattering and absorption is still much less than extinction, indicating that the differences cannot be explained by including absorption.

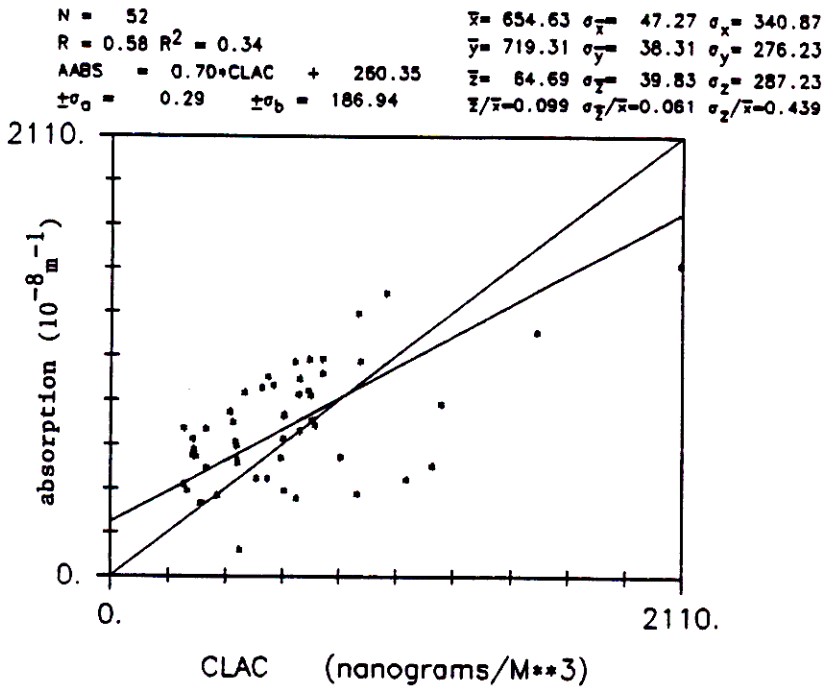

Figure 3F.13: Comparison of the coefficient of absorption by LIPM and light-absorbing (elemental) carbon by TOR. The diagonal line represents the predicted absorption if all particles had absorption efficiency of 10 m^2/g.

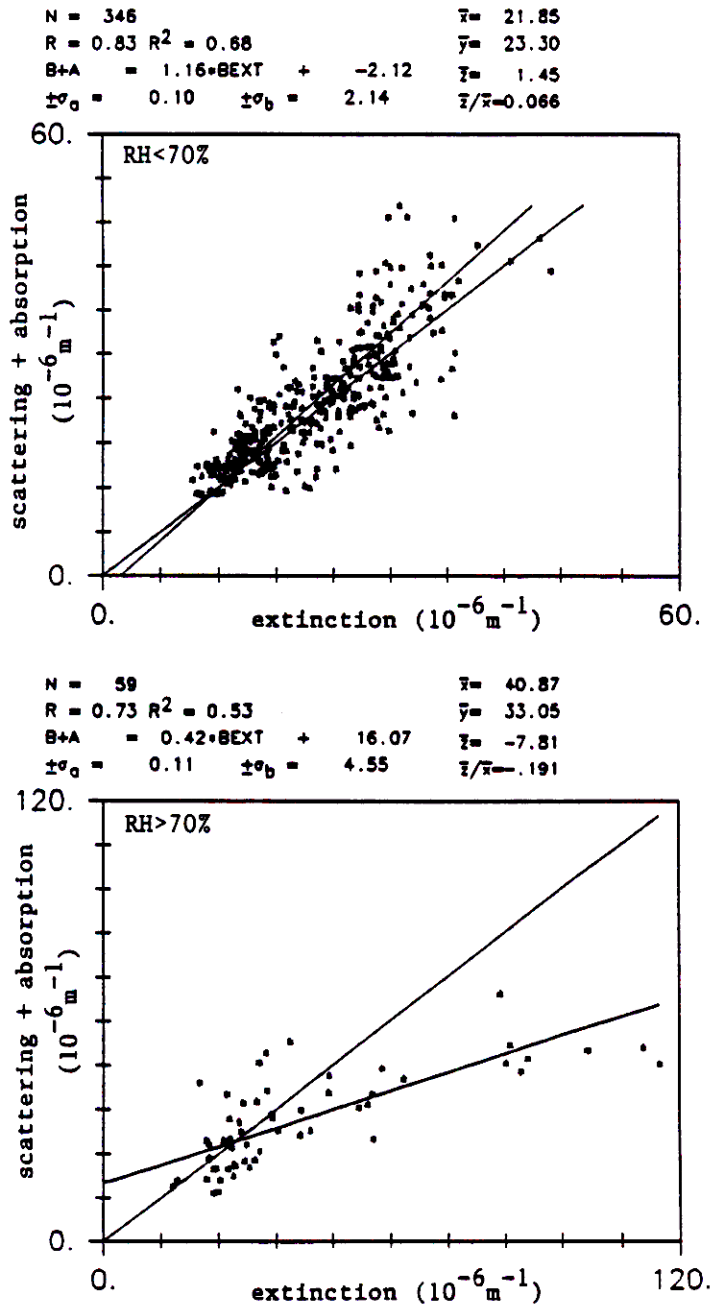

Figure 3F.14: Comparison of 6-hour transmissometer extinction and sum of nephelometer scattering and LIPM absorption for relative humidity below 70% (upper plot) and above 70% (lower plot). All WHITEX sites and time periods.

References

[1]Charlson, R.J., H. Horvath, and R.F. Pueschel, "The direct measurement of atmospheric light scattering coefficient for studies of visibility and pollution," *Atmos. Environ.*, **1**, 469 (1967).

[2]Malm, W.C., and J.V.Molenar, "Visibility measurements in national parks in the western United States," *APCA Journal*, **34**, (9), (1984).

[3]Malm, W.C., "Review of techniques for measuring atmospheric extinction," Paper #86–17.2, presented at the 79th Annual Meeting and Exhibition of the Air Pollution Control Association, June 22–27, 1986, Minneapolis, Minnesota.

[4]OPTEC, Inc., 199 Smith Road, Lowell, Michigan 49331.

[5]Dzubay, T.G., R.K. Steven, C.W. Lewis, D. Hern, W.J. Courtney, J.W. Tesch, and M.A. Mason, "Visibility and aerosol composition in Houston, Texas," *Environ. Sci. and Tech.*, **16**, 514, (1982).

[6]Tombach, I. and D. Allard, "Comparison of visibility measurement techniques: Eastern United States," Report EPRI EA–3292, Electric Power Research Institute, Palo Alto, CA (1983).

[7]Ensor, D.S. and A.P. Waggoner, "Angular truncation error in the integrating nephelometer," *Atmos. Environ.*, **4**, 481, (1970).

[8]Quenzel, H., G.H. Ruppersberg and R. Schellhase, "Calculations about the systematic error of visibility-meters measuring scattered light," *Atmos. Environ.*, **9**, 587, (1975).

[9]Campbell, D., S. Copeland, T. Cahill, R. Eldred, C. Cahill, J. Vesenka, and T. VanCuren, 1989: The coefficient of optical absorption from particles deposited on filters: integrating plate, integrating sphere, and coefficient of haze measurements, *Proceedings of the 82nd Annual Meeting of AWMA*, June 25–30, Anaheim, CA, 89–151.6.

[10]Watson, J.G., J.C. Chow, L.C. Prichett, L.W. Richards, D.L. Dietrich, J. Molenar, J. Faust, S.R. Anderson, and C. Sloane, "Comparison of three measures of visibility extinction in Denver, Colorado," *Proceedings of the 82nd Annual Meeting of AWMA*, June 25–30, 1989, Anaheim, CA, paper 89–151.4.